Analytical Performance of Hybrid Beam Index Modulation

Ali Mokh, Mohamed Shehata, Matthieu Crussière, Maryline Hélard

Analytical Performance of Hybrid Beam Index Modulation

Ali Mokh, Mohamed Shehata, Matthieu Crussière and Maryline Hélard

Univ Rennes, INSA Rennes, CNRS, IETR-UMR 6164, F-35000 Rennes
email:{ali.mokh, mohamad.shehata, mattieu.crussiere, maryline.helard}@insa-rennes.fr

***Abstract*—In this letter, a novel Beam Index Modulation (BIM) architecture with hybrid beamforming is introduced for millimeter-wave (mmWave) communications. Indeed, spatial scattering modulation and BIM have recently been proposed as a potential extension for Spatial Modulation to deal with sparse non Line of Sight channel environments. However, these recent approaches lack complete analyses for practical scenarios. SSM is limited to orthogonal non correlated channel paths and single user up-link scenarios, while BIM was hitherto studied for analog beamforming scenarios in which the interference between the beams is not tackled. Aiming at mitigating such inter-beam interference, we propose in this paper to add a digital precoding layer to the conventional analog-BIM framework, thus leading to a hybrid-BIM scheme. We analyze the performance of such new scheme by deriving the analytic closed form expressions of the achievable spectral efficiency and bit error probability. Simulation results show the validity of our theoretical results and highlight the performance gain brought by the hybrid beamforming strategy applied to BIM mmWave communications.**

***Index Terms*—Beam Index Modulation , Zero Forcing, Hybrid Beamforming, Analog Beamforming, mmWave.**

I. Introduction

Increasing data rates, the spectral efficiency (SE) and the energy efficiency (EE) are considered as the main targets of future wireless networks. This can be achieved by different key enablers such as massive multiple-input multiple-output (MIMO) system architecture and millimeter wave (mmWave) communications. Hardware complexity however remains a major issue to address for the practical implementation of such solutions.

Hybrid beamforming [1] has rapidly emerged as a promising solution to decrease the massive MIMO hardware complexity by utilizing less radio frequency (RF) chains than the number of antenna elements. It has even been shown that employing hybrid beamforming achieves close SE performance compared to the full digital solutions in sparse channels as for example in mmWave systems [1].

Complementary to hybrid beamforming approaches, Index Modulation (IM) has recently been proposed as a low complexity-energy efficient technique for next generation wireless communication systems [2]. IM is the generalization of the ON OFF keying concept applied to a certain dimension, such as frequency (sub-carrier) or space (antenna) for instance.

Specifically, Spatial Modulation (SM) has become a popular index modulation technique applied along the spatial axis, where the index of the transmit or receive antennas codes the useful information [3]–[5]. With the emerging mmWave systems, SM has recently been adapted to sparse scattering propagation conditions. As an example, SM dealing with pure Line of Sight (LoS) channels has been studied in [6], where analog beamforming is implemented at the transmitter.

Another IM technique applied to the spatial domain and referred to as Beam Index Modulation (BIM) has very recently been proposed [7]. The idea behind BIM is to exploit the multiple path scattering in a given channel by mapping the information bits onto the indexes of the beams associated to the propagation paths that can be established between the transmitter and the receiver. In other words, a given M-ary symbol is transmitted when activating one given propagation path out of M possible ones. Clearly, path activation relies on beamforming capacilities at both the transmitter and the receiver. In [7], the authors restrained the study to the simple case of analog beamforming, thus suffering from potential inter-beam interference.

In this letter, we extend the BIM approach by making use of a hybrid beamforming architecture instead of the pure analog one, where the additional digital precoder aims at mitigating the inter-beam interference. We provide analytical derivations for the SE and Bit Error Probability (BEP) expressions of the proposed hybrid-BIM system when applying the zero forcing (ZF) criterion to the digital precoder. We then highlight the enhancement provided by the hybrid-BIM approach compared to the pure analog-BIM one.

II. System Model

In this section, we set up the complete model for a communication system utilizing the BIM scheme with hybrid beamforming.

A. MIMO System Model with hybrid beamforming

A MIMO system equipped with N_t transmit antennas and N_r receive antennas is considered and can be modeled as follows:

$$\mathbf{y}=\mathbf{F}_r\mathbf{H}\underbrace{\Delta\mathbf{F_t}\mathbf{W}\mathbf{x}}_{\mathbf{s}}+\mathbf{F}_r\mathbf{n}, \tag{1}$$

where $\mathbf{H}\in\mathbb{C}^{N_r\times N_t}$ is the MIMO flat fading channel matrix with elements $h_{j,i}$ representing the complex channel gain between the ith transmit antenna, denoted T_i, and the jth receive antenna, denoted R_j. $\mathbf{s}\in\mathbb{C}^{N_t\times 1}$ is the vector of samples transmitted through the N_t transmit antennas. $\mathbf{y}\in\mathbb{C}^{N_r\times 1}$ is the vector of the received signals. $\mathbf{F}_t\in\mathbb{C}^{N_t\times L_t}$ is the analog beamformer at the transmitter, such that L_t is the number of RF chains at the transmitter. Throughout this letter we assume that the number of transmit and receive RF chains equals the number of the selected paths (transmit beams) $L_t=L_r=N_p$. $\mathbf{W}\in\mathbb{C}^{L_t\times N_p}$ is the digital ZF precoder used to annihilate the inter-beam interference. $\mathbf{F}_r\in\mathbb{C}^{N_p\times N_r}$ is the analog beam combiner at the receiver. $\mathbf{n}\in\mathbb{C}^{N_r\times 1}$ is the vector of additive white Gaussian noise (AWGN) samples η_j such that $\eta_j\sim\mathcal{CN}(0,\sigma_n^2)$ given that σ_n^2 represents the noise variance. Finally, $\Delta\in\mathbb{R}^{N_p\times N_p}$ is a diagonal scaling matrix of entries $\delta_j, j\in[1,N_p]$ which ensures the normalization of the transmitted power after hybrid beamforming. We hence have:

$$\delta_j=\frac{1}{\sqrt{\mathrm{Tr}\Big((\mathbf{F}_t\mathbf{W}\mathbf{x_j})^H\mathbf{F}_t\mathbf{W}\mathbf{x_j}\Big)}}. \tag{2}$$

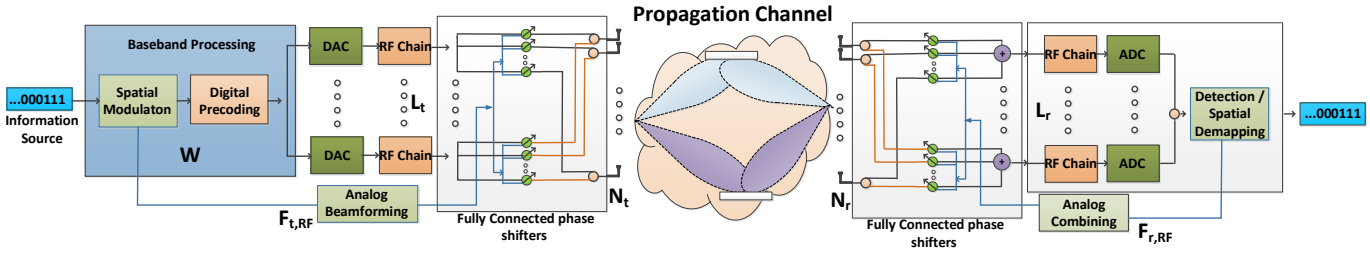

Figure 1: Block diagram of BIM with analog beamforming architecture

B. Beam Index Modulation

The spatial symbol $\mathbf{x}_k$ where k is the index of the beam that should be targeted according to the spatial mapping, are formed such that the entries $x_k(j)$ of $\mathbf{x}_k$ verify $x_k(j)=1$ for $j=k$ and $x_k(j)=0, \forall j \neq k$. A group of $m=\log_2(N_p)$ bits, where N_p is the number of paths (transmit-receive beam pairs), are mapped onto a spatial symbol $\mathbf{x}_k \in \mathbb{N}^{N_p \times 1}$ written as $\mathbf{x}_k = \begin{bmatrix} 0 & \dots & \underbrace{1}_{k-thposition} & \dots & 0 \end{bmatrix}^T$ given that k represents the targeted beam. Then, the analog and digital beamforming matrices $\mathbf{F}_t\mathbf{W}$ transforms the vector of spatial symbols $\mathbf{x}$ into the vector of transmitted samples $\mathbf{s} \in \mathbb{C}^{N_t \times 1}$.

At the receiver side, the BIM receiver has to detect the targeted beam using analog beam combining. The block diagram of the analog beamforming BIM system is depicted in Fig. 1.

III. Channel Model and Beamforming

Throughout this letter, we use the sparse geometric channel model detailed in [8]. Then, the active path selection is done at both the transmitter and the receiver through beam training and beam alignment steps [9]. The channel matrix for each path (transmit-receive beam pair) p is represented as follows:

$$\mathbf{H}_p = \sqrt{N_t N_r}\alpha_p \mathbf{a}_r(\theta_p)\mathbf{a}_t^H(\phi_p), \tag{3}$$

where α_p is the complex amplitude of propagation path p which is one of the N_p chosen, such that $\mathbb{E}[|\alpha_p|^2]=\hat{\alpha}$. ϕ_p represents the Angle of Departure (AoD) for path p, such that $\phi_p \in [0,2\pi]$. θ_p represents the Angle of Arrival (AoA) for path p, such that $\theta_p \in [0,2\pi]$. Finally, $\mathbf{a}_t(\phi_p)$ and $\mathbf{a}_r(\theta_p)$ are the transmit array and receive array steering vectors respectively, which depend on the array geometry. In this letter, we use Uniform Linear Array (ULA) for transmit and receive arrays. Henceforth, the steering vectors $\mathbf{a}_t(\phi_p)$ and $\mathbf{a}_r(\theta_p)$ are defined as:

$$\mathbf{a}_t(\phi_p) = \frac{1}{\sqrt{N_t}}[1, e^{j\gamma(\phi_p)}, \dots, e^{j(N_t-1)\gamma(\phi_p)}]^T, \tag{4}$$

$$\mathbf{a}_r(\theta_p) = \frac{1}{\sqrt{N_r}}[1, e^{j\zeta(\theta_p)}, \dots, e^{j(N_r-1)\zeta(\theta_p)}]^T, \tag{5}$$

such that $\gamma(\phi_p)$ is represented as $\gamma(\phi_p) = \frac{2\pi}{\lambda} d_t \sin(\phi_p)$ and $\zeta(\theta_p)$ is given as $\zeta(\theta_p) = \frac{2\pi}{\lambda} d_r \sin(\theta_p)$, where λ is the wavelength of the signal, and d_t and d_r are the inter-element antenna spacing at the transmitter and the receiver respectively.

A. Analog Beamforming and Combining Technique

In the proposed scheme, the analog beamformer and combiner are designed in order to align the transmit and receive beams to discriminate between different paths of the channel, where the selection of the path is related to the transmitted symbol using BIM. As aforementioned, only the most dominant N_p channel paths are chosen for transmission, such that N_p is chosen to satisfy certain hardware constraints $N_p \leq \min(L_t, L_r)$. The dominant paths are estimated using conventional beam training techniques [9].

Therefore, the analog beamformer at the transmitter side is calculated as follows $\mathbf{F}_t = [\mathbf{a}_t(\phi_i)]_{i=[1:N_p]}$. Also, the analog beam combiner is calculated at the receiver side as follows $\mathbf{F}_r = [\mathbf{a}_r(\theta_i)^H]_{i=[1:N_p]}$. Furthermore, the equivalent channel $\mathbf{H}_e$ is calculated as: $\mathbf{H}_e = \mathbf{F}_r\mathbf{H}\mathbf{F}_t$. Finally, the ZF precoder is calculated as $\mathbf{W} = \mathbf{H}_e^H(\mathbf{H}_e\mathbf{H}_e^H)^{-1}$ for the inter-beam interference mitigation.

IV. Analytical Performance Analysis

A. Spectral Efficiency

The analog beamformer at the transmitter $\mathbf{F}_t$ and combiner at the receiver $\mathbf{F}_r$ aim at normalizing the spatial phases of $\mathbf{H}_p$, so that, the p-th term in the equivalent channel's diagonal, which represents the channel gain at path p, can be expressed as:

$$|\mathbf{H}_e(p,p)| = |\mathbf{F}_r^p \mathbf{H}_p \mathbf{F}_t^p| = \frac{1}{\sqrt{N_t N_r}} \sum_{i=1}^{N_t}\sum_{i=1}^{N_r} |\alpha_p| = \sqrt{N_t N_r}|\alpha_p|. \tag{6}$$

In (6), one can observe the cancellation of the phase effects arising from the channel spatial dimensions (AoD and AoA) through beam alignment, ending up with the amplitude of the channel gain $|\alpha_p|$ scaled by the transmit and receive antenna array gains $\sqrt{N_t N_r}$. On that basis, the equivalent channel $\mathbf{H}_e$ can statistically be analyzed by splitting the diagonal and off-diagonal parts and tackling each one separately. Considering the diagonal term in (6), and assuming that the channel complex values α are independent and identically distributed (i.i.d) complex Gaussian $\alpha \sim \mathcal{CN}(0,1)$, we can conclude that $|\alpha|$ follows a Rayleigh distribution with mean $\frac{\sqrt{\pi}}{2}$ and variance $1-\frac{\pi}{4}$. Therefore, we have:

$$|\mathbf{F}_r^p \mathbf{H}_p \mathbf{F}_t^p| \sim \mathbf{Rayleigh}\left(\frac{\sqrt{\pi N_t N_r}}{2}, N_t N_r (1-\frac{\pi}{4})\right). \tag{7}$$

Also, each off diagonal term $\mathbf{F}_r^p \mathbf{H}_p \mathbf{F}_t^{y \neq p}$ is as follows:

$$|\mathbf{F}_r^p \mathbf{H}_p \mathbf{F}_t^{y \neq p}| = \sqrt{N_r}|\alpha_p| \sum_{i=1}^{N_t} |\mathbf{a}_t^H(\phi_p)\mathbf{a}_t(\phi_y)| \tag{8}$$

Given that ϕ is uniformly distributed in $[0,2\pi]$, $d_t = \frac{\lambda}{2}$ and that ϕ and α are statistically independent, the expected value of the off-diagonal term $\mathbb{E}\left\{|\mathbf{F}_r^p \mathbf{H}_p \mathbf{F}_t^{y \neq p}|\right\}$ can be expressed according to [10] as follows:

$$\begin{aligned} \mathbb{E}\left\{|\mathbf{F}_r^p \mathbf{H}_p \mathbf{F}_t^{y \neq p}|\right\} &= \sqrt{N_r}\mathbb{E}\{|\alpha_p|\}\mathbb{E}\left\{\sum_{i=1}^{N_t} |\mathbf{a}_t^H(\phi_p)\mathbf{a}_t(\phi_y)|\right\} \\ &= \frac{\sqrt{N_r \pi}}{2N_t} \sum_{i=1}^{N_t} J_0^2(\pi(i-1)) \end{aligned} \tag{9}$$

where $J_0(x)$ is the zero order Bessel function of x and it decays in magnitude proportional to $\frac{1}{\sqrt{x}}$, which means that $J_0^2(x)$ decays in magnitude proportional to $\frac{1}{x}$. Therefore, from equations(7) and (9) the off diagonal term can be assumed to be negligible compared to the diagonal ones when N_t is large enough. Moreover, the off diagonal term is proved in [10] to approach 0, when $N_t \to \infty$ leading to the favourable propagation. Henceforth, considering the diagonal elements only, for tractability, the calculated SE can be considered as an upper bound for our framework.

Proposition 1: The average per stream SE upper bound can be approximated by:

$$\mathcal{C}_p \approx \frac{2}{\ln 2}\left(\ln(\sqrt{\rho N_t N_r}\sigma) + \frac{\ln(2)}{2} - \frac{\kappa}{2}\right) \tag{10}$$

where ρ is the Signal to Noise Ratio (SNR), and $\kappa \approx 0.5772$ is the Euler constant.

Proof: This upper bound for per stream SE can be asymptotically achieved with increasing N_t and is represented as follows:

$$\begin{aligned}\mathcal{C}_p &= \mathbb{E}\{\log_2(1+\rho|\mathbf{F}_r^p \mathbf{H}_p \mathbf{F}_t^p|^2)\} \\ &= \mathbb{E}\{\log_2(1+\rho N_t N_r |\alpha_p|^2)\}.\end{aligned} \tag{11}$$

Assuming that $\rho N_t N_r >> 1$, which is a valid assumption in mmWave massive MIMO systems, then $1 + \rho N_t N_r |\alpha_p|^2 \approx \rho N_t N_r |\alpha_p|^2$. Therefore, the per stream SE upper bound can be expressed as:

$$\mathcal{C}_p \approx \frac{2}{\ln 2}\mathbb{E}\left\{\ln\left(\sqrt{\rho N_t N_r}|\alpha_p|\right)\right\} \tag{12}$$

where $\ln\left(\sqrt{\rho N_t N_r}|\alpha_p|\right)$ has a Log-Rayleigh distribution defined in [11] ($\ln\left(\sqrt{\rho N_t N_r}|\alpha_p|\right) \sim \mathbf{LogRay}(\rho N_t N_r \sigma^2)$) , where σ^2 is the variance of the complex Gaussian channel coefficients α. Then, the Probability Density Function (PDF) of $z = \ln\left(\sqrt{\rho N_t N_r}|\alpha_p|\right)$ is given as follows [11]:

$$f(z) = \frac{(e^z)^2}{\sigma_z^2}\exp\left(-\frac{(e^z)^2}{2\sigma_z^2}\right) \tag{13}$$

where σ_z^2 results from scaling σ^2 by $\rho N_t N_r$ ($\sigma_z = \rho N_t N_r \sigma^2$). Moreover, the mean ($\mu$) and variance ($\eta^2$) of $\ln\left(\sqrt{\rho N_t N_r}|\alpha_p|\right)$ are expressed as [11], [12]: $\mu = \ln(\sqrt{\rho N_t N_r}\sigma) + \frac{\ln(2)}{2} - \frac{\kappa}{2}$ and $\eta^2 = \frac{\pi^2}{24}$. Therefore, the average per stream SE upper bound in can be expressed as in (12). ■

B. Conditional Bit Error Probability

The detector has to analyze the received signals:

$$\forall j, \quad y_j = \begin{cases} \delta_j + u_j & \text{, if } j^{th} \text{ beam is targeted} \\ u_j & \text{, otherwise} \end{cases} \tag{14}$$

where u_j is the received noise at beam j after applying the analog combiner, given that $\mathbf{u} = \mathbf{F}_r \mathbf{n}$ and $\mathbf{u} \in \mathbb{C}^{N_p \times 1}$. Then, the formula that derives the analytic average BEP conditioned by the channel $\mathcal{P}_e$ for BIM schemes is:

$$\mathcal{P}_e = \frac{1}{m} \cdot \mathbb{E}\left\{\sum_{k}^{N_p}\sum_{j \neq k}^{N_p} \mathcal{P}(\mathbf{x}_k \to \mathbf{x}_j) d(\mathbf{x}_k, \mathbf{x}_j)\right\}. \tag{15}$$

where $d(\mathbf{x}_k, \mathbf{x}_j)$ is the Hamming distance between two spatial symbols $\mathbf{x}_k$ and $\mathbf{x}_j$, and $\mathcal{P}(\mathbf{x}_k \to \mathbf{x}_j)$ is the Pairwise Error Probability (PEP) between $\mathbf{x}_k$ and $\mathbf{x}_j$.

Proposition 2: Considering the Maximum Likelihood (ML) detection, the PEP of the BIM scheme conditioned by the knowledge of the channel matrix $\mathbf{H}$ is approximated by:

$$\mathcal{P}(\mathbf{x}_k \to \mathbf{x}_j|\mathbf{H}) \approx Q\left(\frac{-j}{2\sigma_n}\right) \tag{16}$$

Proof: The PEP writes as,

$$\begin{aligned}&\mathcal{P}(\mathbf{x}_k \to \mathbf{x}_j|\mathbf{H}) = \mathcal{P}(d_k > d_j|\mathbf{H}) \\ &= \mathcal{P}((u_j\delta_j - u_k\delta_j) > \frac{1}{2}(2{\delta_j}^2)|\mathbf{H}) = Q(\sqrt{\xi})\end{aligned} \tag{17}$$

where $d_j = \|\mathbf{y} - \delta_j \mathbf{x}_j\|^2$ and $Q(x)$ is the Gaussian distribution function: $Q(r) = \int_x^\infty \frac{1}{2\pi} e^{-\frac{r^2}{2}} dr$ and ξ is calculated as follows:

$$\xi = \frac{\delta_j^2}{2\left\|\mathbf{F}_r^k - \mathbf{F}_r^j\right\|^2 \sigma_n^2}, \tag{18}$$

where,

$$\left\|\mathbf{F}_r^k - \mathbf{F}_r^j\right\|^2 = \frac{1}{N_r}\sum_{b=1}^{N_r}(e^{jb\theta_k} - e^{jb\theta_j})^2 \tag{19}$$

For high numbers of receive antennas, the analog combiners at the receiver become orthogonal. Thus, we can write $\left\|\mathbf{F}_r^k - \mathbf{F}_r^j\right\|^2 \approx 2$. Then we have $\xi = \frac{\delta_j^2}{4\sigma_n^2}$, which concludes the proof. ■

C. Multistream ABER

Proposition 3: The multistream Average BEP (ABEP) of BIM transmission in a Rayleigh fading channel is approximated by:

$$\mathbf{ABEP} \approx \frac{1}{2}\sqrt{\frac{\mu}{1+\mu}} \tag{20}$$

where $\mu = \frac{N_t N_r}{4\sigma_n^2}$.

Proof:

When the channel H changes, the value of ξ changes. Assume that the channel matrix entries follow a Rayleigh distribution in amplitude, i.e. α follows a Rayleigh distribution. For δ_j, considering the best case to find the lower bound of the Average BEP (ABEP), where for high number of transmit antennas, the interference at the off diagonal terms in the equivalent channel matrix is zero, in this case δ_j could be approximated by the diagonal terms:

$$\delta_j = \mathbf{H}_e(j,j) = \sqrt{N_t N_r}\alpha_j. \tag{21}$$

Than we can easily see that:

$$\xi = \frac{N_t N_r \alpha_j}{4\sigma_n^2} = \mu\alpha^2 \tag{22}$$

follows a chi squared distribution where the PDF is:

$$p(\xi) = \frac{1}{\mu}e^{\frac{-\xi}{\mu}}, \quad \xi > 0 \tag{23}$$

and as a result, using the same mathematical derivations used to compute the ABEP of BPSK in Rayleigh channels, the ABEP is given by:

$$\int_0^{+\infty} Q(\sqrt{\xi})p(\xi)d\xi = \frac{1}{2}\sqrt{\frac{\mu}{1+\mu}} \tag{24}$$

■

V. Simulation Results

In this section, the performance of the proposed hybrid-BIM scheme is evaluated in terms of SE and BER. The transmit and receive antenna arrays are ULAs, and the number of transmit/receive RF chains equals the number N_p of the active sparse channel paths. Finally, we consider that perfect Channel State Information (CSI) is available at both the transmitter and the receiver.

In Fig. 2, we first compare the empirical probability density function (PDF) of $\ln\left(\sqrt{\rho N_t N_r}|\alpha_p|\right)$ with the theoritical PDF obtained from the Log-Rayleigh distribution in (13) for validation purpose.

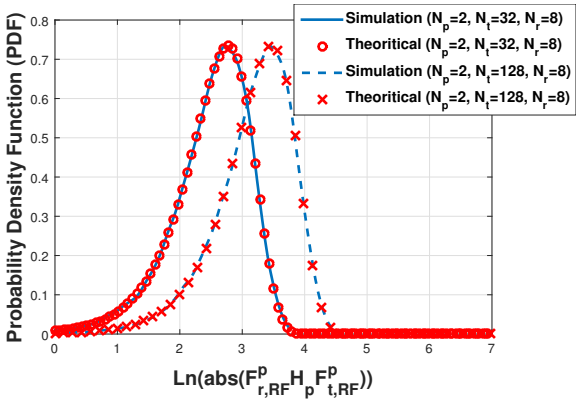

Figure 2: Empirical and theoretical PDF of $\ln(|\mathbf{F}_r^p\mathbf{H}_p\mathbf{F}_t^p|)$ for different multiantenna scenarios.

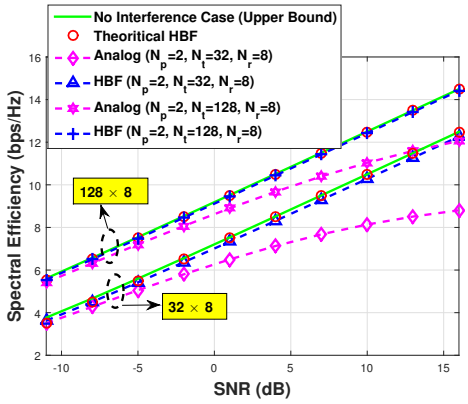

Figure 3: Comparing the per stream SE for the analog and hybrid beamforming scenarios in a sparse nLoS channel environment.

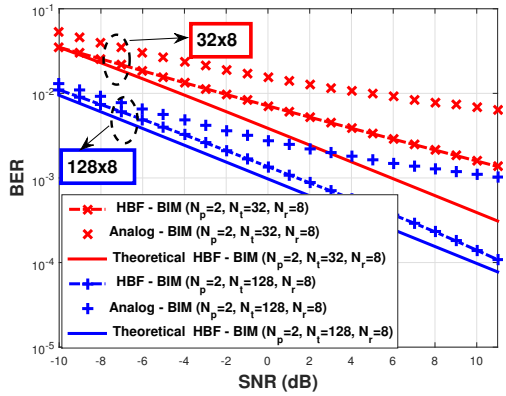

Figure 4: Comparing the BER for different analog and hybrid beamforming BIM scenarios in a sparse nLoS channel environment.

In Fig. 3, the performance of the proposed hybrid-BIM is evaluated through the measurement of the SE versus the ratio between the average transmit power level and noise level, i.e. SNR=$\frac{\bar{P}_t}{\sigma_n^2}$. Two system configurations, namely 32x8 with $N_p = 2$ paths and 128x8 with $N_p = 2$ paths, are considered. It is observed that the numerical results are upper bounded by the theoretical ones for all setups and almost match asymptotically (N_t is large), hence validating the derived SE model in Proposition 1. Moreover, the analog-BIM scheme is compared to the hybrid-BIM one for both setups. It is concluded that the hybrid approach achieves higher SE compared to the pure analog one. One can also note that the SE gap between them increases when the SNR level is raised. This is easily explained from the beam-interference level which is not cancelled with analog-BIM and thus limits the performance at high SNR regime.

In Fig. (4), the performance of the proposed system is evaluated in terms of BER versus SNR and using the same system configurations as previously. The theoretical ABEP given by Proposition 3 is compared to the simulated BEP of BIM using either hybrid or analog beamforming. Again from its beam-interference cancellation capability, it is clearly seen that the hybrid-BIM scheme outperforms the analog-BIM one, as more as the SNR level increases. On one other hand, it is shown that the theoretical BEP of the hybrid-BIM system becomes accurate when sufficiently increasing the number of transmit antennas. This comes from the approximation made in Proposition 3, where a high number of transmit antennas is considered to neglect the off-diagonal elements of the equivalent channel.

VI. Conclusion

In this letter, BIM with hybrid beamforming at the transmitter and analog combining at the receiver is introduced and studied in a mmWave context. Analytical derivations of the SE and BEP of the proposed hybrid-BIM scheme are provided. Thereby, it is shown that the hybrid-BIM approach increases the system SE and reduces the transmission BER compared to the pure analo- BIM case of the literature. More precisely, it is highlighted that the proposed hybrid-BIM scheme outperforms the analog-BIM one at high SNR, since the latter may be strongly affected (dominated) by inter-beam interference.

References

[1] A. Alkhateeb, O. E. Ayach, G. Leus, and R. W. Heath, "Channel estimation and hybrid precoding for millimeter wave cellular systems," *IEEE Journal of Selected Topics in Signal Processing*, vol. 8, no. 5, pp. 831–846, Oct 2014.

[2] E. Basar, M. Wen, R. Mesleh, M. Di Renzo, Y. Xiao, and H. Haas, "Index modulation techniques for next-generation wireless networks," *IEEE Access*, vol. 5, pp. 16 693–16 746, 2017.

[3] M. Di Renzo, H. Haas, A. Ghrayeb, S. Sugiura, and L. Hanzo, "Spatial modulation for generalized mimo: Challenges, opportunities, and implementation," *Proceedings of the IEEE*, vol. 102, no. 1, pp. 56–103, 2014.

[4] A. Mokh, M. Crussière, M. Hélard, and M. Di Renzo, "Theoretical performance of coherent and incoherent detection for zero-forcing receive antenna shift keying," *IEEE access*, vol. 6, pp. 39 907–39 916, 2018.

[5] A. Mokh, M. Hélard, and M. Crussiere, "Extended receive spatial modulation mimo scheme for higher spectral efficiency," in *2018 IEEE 87th Vehicular Technology Conference*, 2018.

[6] P. Liu, M. D. Renzo, and A. Springer, "Line-of-sight spatial modulation for indoor mmwave communication at 60 ghz," *IEEE Transactions on Wireless Communications*, vol. 15, no. 11, pp. 7373–7389, Nov 2016.

[7] Y. Ding, V. Fusco, A. Shitvov, Y. Xiao, and H. Li, "Beam index modulation wireless communication with analog beamforming," *IEEE Transactions on Vehicular Technology*, pp. 1–1, 2018.

[8] A. Alkhateeb, G. Leus, and R. W. Heath, Jr, "Limited Feedback Hybrid Precoding for Multi-User Millimeter Wave Systems," *ArXiv e-prints*, Sep. 2014.

[9] Y. M. Tsang, A. S. Y. Poon, and S. Addepalli, "Coding the beams: Improving beamforming training in mmwave communication system," in *2011 IEEE Global Telecommunications Conference - GLOBECOM 2011*, Dec 2011, pp. 1–6.

[10] X. Wu, N. C. Beaulieu, and D. Liu, "On favorable propagation in massive mimo systems and different antenna configurations," *IEEE Access*, vol. 5, pp. 5578–5593, 2017.

[11] B. Rivet, L. Girin, and C. Jutten, "Log-rayleigh distribution: A simple and efficient statistical representation of log-spectral coefficients," *IEEE Transactions on Audio, Speech, and Language Processing*, vol. 15, no. 3, pp. 796–802, March 2007.

[12] X. Wu, H. Haas, and P. M. Grant, "Cooperative spatial modulation for cellular networks," *IEEE Transactions on Communications*, vol. 66, no. 8, pp. 3683–3693, Aug 2018.